

# Abnormal Cardiac Rhythm Detection Based on Photoplethysmography Signals and a Recurrent Neural Network

Loïc Jeanningros<sup>1,2</sup>, Jérôme Van Zaen<sup>1</sup>, Clémentine Aguet<sup>1,2</sup>, Mathieu Le Bloa<sup>3</sup>, Alessandra Porretta<sup>3</sup>, Cheryl Teres<sup>3</sup>, Claudia Herrera<sup>3</sup>, Giulia Domenichini<sup>3</sup>, Patrizio Pascale<sup>3</sup>, Adrian Luca<sup>3</sup>, Jorge Solana Muñoz<sup>3</sup>, Jean-Marc Vesin<sup>2</sup>, Jean-Philippe Thiran<sup>2</sup>, Etienne Pruvot<sup>3</sup>, Mathieu Lemay<sup>1</sup>, Fabian Braun<sup>1</sup>

<sup>1</sup>Swiss Center for Electronics and Microtechnology (CSEM), Neuchâtel, Switzerland

<sup>2</sup>Swiss Federal Institute of Technology Lausanne (EPFL), Lausanne, Switzerland

<sup>3</sup>Lausanne University Hospital (CHUV), Lausanne, Switzerland

## Abstract

*Wearable devices based on photoplethysmography (PPG) allow for the screening of large populations at risk of cardiovascular disease. While PPG has shown the ability to discriminate atrial fibrillation (AF) – the most common cardiac arrhythmia (CA) – versus normal sinus rhythm, it is not clear whether such AF detectors are efficient in presence of CAs other than AF.*

*We propose to apply a simple recurrent neural network (RNN) on a newly acquired dataset containing eight different types of CAs. The classifier takes sequences of inter-beat intervals (IBIs) as input and discriminates between normal and abnormal rhythm.*

*The RNN achieved 84% accuracy in detecting abnormal rhythms. Some CAs were well detected (AF: 99.6%; atrial tachycardia: 100%), whereas other CAs were more difficult to detect (atrial flutter: 65.4%; bigeminy: 72.4%; ventricular tachycardia 80%).*

*This study shows the potential of PPG technology to detect not only AF but also other types of CA. It highlights the strengths and weaknesses of IBI-based detection of abnormal rhythms and paves the way towards continuous monitoring of CAs in everyday life.*

## 1. Introduction

Cardiac Arrhythmias (CAs) are a critical health problem associated with a variety of complications, such as stroke or heart failure [1]. A large prospective cohort in the United Kingdom estimated that 3.6% of males and 1.6% of females aged from 55 to 64 years are suffering from rhythm abnormality [2]. For people over 65 years, 6.6% of males and 3.2% of females are affected [2]. Since CAs are often asymptomatic and intermittent during their early stages [3], [4], continuous monitoring is indicated to screen large at-risk populations. In this context, wearable devices

based on photoplethysmography (PPG) appear well-suited, as they are unobtrusive and accessible. Hence, early detection of arrhythmias could enable effective prevention strategies to avoid complications such as strokes or heart failure.

Many studies demonstrated good performance for the PPG-based detection of atrial fibrillation (AF) [5]. However, AF patients account for only half of all patients with CAs. It is therefore essential to consider other types of CA for robust monitoring solutions. A few studies have investigated the detection of atrial flutter [6], [7], ventricular tachycardia [8], [9], premature contractions [7], [9]–[11] and atrioventricular block [11] in addition to AF. Only Liu et al. [9] have tackled the problem as a whole by classifying PPG segments into six different classes of CA with a deep convolution neural network. However, deep learning models require large annotated datasets for training. They come with an intrinsic lack of interpretability and require high computational resources, two serious drawbacks for wearable embedded medical devices.

In this study, we propose a simple recurrent neural network that takes series of inter-beat intervals (IBIs) as input to perform a binary classification – normal versus abnormal – on PPG-signals containing eight different types of CAs.

## 2. Material and Methods

### 2.1. Dataset

64 patients referred for diagnostic or therapeutic electrophysiological procedures at the Lausanne University Hospital (CHUV) were included. This study received approval from the local ethics committee of Lausanne (CER-VD, Project-ID 2021-00586) and has been registered on ClinicalTrials.gov (NCT04884100).

PPG signals were recorded at 100 Hz from a proprietary

wrist-bracelet (CSEM, Neuchâtel, Switzerland). Simultaneously, 12-lead ECG signals were acquired with the Axiom Sensis XP<sup>®</sup> System (Siemens<sup>®</sup>, Munich, Germany) at a sampling frequency of 2 kHz and bandpass-filtered between 0.5 and 200 Hz. The system provided R-peak annotations, indicating the occurrence of heartbeats.

ECG signals were manually annotated by a medical expert to identify CAs. Both atrial and ventricular bigeminy, as well as trigeminy and quadrigeminy, or any combination of these rhythms, were indistinctly labeled as bigeminy (B). The label AVRT included both atrioventricular reentrant tachycardia and atrioventricular nodal reentrant tachycardia. Finally, single atrial and ventricular extrasystoles were labelled beat per beat only during normal rhythms.

## 2.2. Classification

The first step to detect abnormal rhythms was to detect pulses in the PPG data with the *qppg\_fast* detector [12], [13], and compute the corresponding IBIs. This detector has shown best performance to detect heartbeats in presence of CAs [14]. Then, 30-second windows of IBIs were extracted. The reference rhythm label for each window was determined from the ECG annotations. Windows collected during ablation or pacing were excluded. The windows labeled as SR or sinus bradycardia (SB) were considered normal while the ones labeled with any other rhythm were considered abnormal (see Table 1). In addition, SR and SB windows with more than four extrasystoles were also considered abnormal.

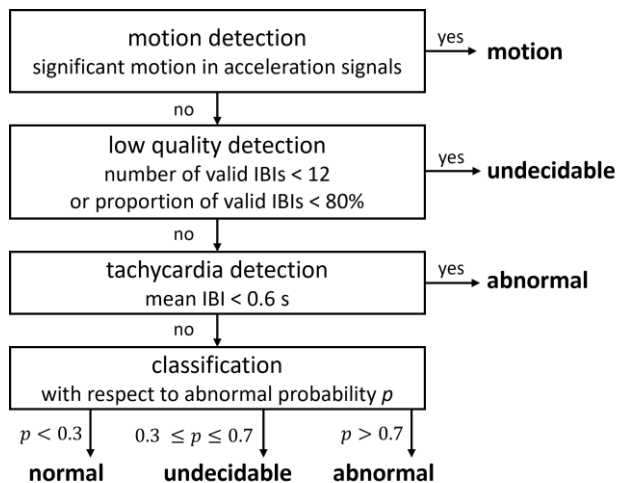


Figure 1. Classification pipeline. Outputs of the classification model are written in bold.

Then, the IBIs in each window were marked as valid if they were between 0.25 and 3 s and their associated quality index – based on PPG pulse morphology – was above 0.75. A recurrent neural network (RNN) was applied to the valid IBIs in each window to determine the probability of

abnormal rhythm. This RNN – composed of a GRU layer and a sigmoid layer – has already demonstrated the ability to classify AF versus SR [15]. It was trained on five datasets where IBIs were extracted from ECG-signals (three PhysioNet datasets [16] and two internal datasets). The mean IBI per window was computed from the valid IBIs. Finally, each window was classified according to the procedure described in Figure 1.

The “undecidable” classification was used to indicate windows for which it was impossible to obtain a reliable decision. Windows classified as either motion or undecidable were excluded before computing the following metrics: accuracy, true positive rate (TPR), true negative rate (TNR), positive predictive value (PPV), negative predictive value (NPV), and F1 score.

## 3. Results

### 3.1. Dataset

45 males and 19 females, with a mean age of  $55.9 \pm 16.0$  years have been included in the clinical study. Eight different types of CA, in addition to normal sinus rhythm (SR) have been recorded and segmented into 9835 homogeneous 30-s windows. The number of subjects and windows are detailed in Table 1 for each type of CA.

Table 1. Details of available cardiac arrhythmias. AV stands for atrioventricular.

	Label	Cardiac arrhythmia	Subjects	Windows
Normal	SR	Sinus rhythm	62	4302
	SB	Sinus bradycardia	39	1894
Abnormal	AF	Atrial fibrillation	13	772
	AFL	Atrial flutter	9	879
	AT	Atrial tachycardia	3	136
	AVB	AV block	2	41
	AVRT	AV re-entrant tachy.	7	36
	B	Bigeminy	9	447
	FE	Frequent extrasystole	54	1036
VT	Ventricular tachy.	7	292	

### 3.2. Classification

1665 windows were removed based on motion analysis leaving 8170 windows usable for classification. The recurrent neural network predicted 2647 windows (32.4%) as undecidable, that is 30.5% of normal windows and 35.3% of abnormal windows.

Classification outputs are detailed in Table 2 for each CA. Among normal rhythms, SR has been correctly classified as normal in 86.4% of cases, and sinus

bradycardia 93.5% of the time. Among abnormal rhythms, atrial fibrillation (99.6%), atrial tachycardia (100%), atrioventricular blocks (93.1%) and atrioventricular re-entrant tachycardia (96.4%) were well classified. Ventricular tachycardia (80.2%), bigeminy (72.4%), atrial flutter (65.4%) and frequent extrasystoles (65.9%) were more difficult to detect.

Table 2. Classifier outputs per cardiac arrhythmia

Label	Normal (%)	Abnormal (%)	# windows
SB	93.5	6.5	796
SR	86.4	13.6	2664
AF	0.4	99.6	486
AFL	34.6	65.4	431
AT	0.0	100.0	48
AVB	6.9	93.1	29
AVRT	3.6	96.4	28
B	27.6	72.4	221
FE	34.1	65.9	643
VT	19.8	80.2	177

Overall, the accuracy of the RNN was 84%. TPR was 77.3% and TNR 88%. PPV was 79.4%, NPV 86.7% and  $F_1$  score 78.4%.

#### 4. Discussion

The simple RNN applied to 30-s windows of IBIs extracted from PPG signals has correctly classified abnormal rhythms like atrial fibrillation, atrial tachycardia, and AV re-entrant tachycardias for more than 96% of windows. Performance was lower for other CAs, like atrial flutter, frequent extrasystoles and bigeminy that were wrongly classified more than 27% of the time. Most episodes of atrial flutter and ventricular tachycardia that remained undetected show series of very regular IBIs. Bigeminy can also be very challenging to detect in the case where premature contractions are systematically miss detected by the pulse detector as shown in Figure 2. In this situation, the resulting sequence of long IBIs is very regular, and misleads the classifier.

Our study is limited by the nature of the dataset, in hospital settings. Patients were undergoing cardiac interventions with intracardiac manipulations. It resulted in an increased number of extrasystoles compared to normal conditions. The significant rate of misclassified SR windows (13.6%) is mostly due to the presence of extrasystoles. The ability of the classifier to detect windows containing more than four extrasystoles (FE) is also very low (65.9%). We hypothesize that, in presence of extrasystoles, sequences of IBIs extracted from PPG-signals are different from those extracted from ECG-signals as shown in Figure 3. Then, the classifier might suffer from being trained on ECG IBIs.

Our classifier achieved 84% accuracy while the deep

convolutional network of Liu et al. [9] reached 97.8% accuracy for the binary classification. Apart from the difference in both training and test datasets, such good performance are probably due to the ability of the neural network to capture morphological characteristics of PPG pulses [9]. Our classifier is obviously limited by taking as input only IBIs. It would be interesting to integrate information about the morphology of individual PPG pulses. The discrimination of bigeminy and extrasystoles would certainly benefit from this additional input and raise classification performance closer to state-of-the-art results, while keeping the classification model suitable for embedding in medical device.

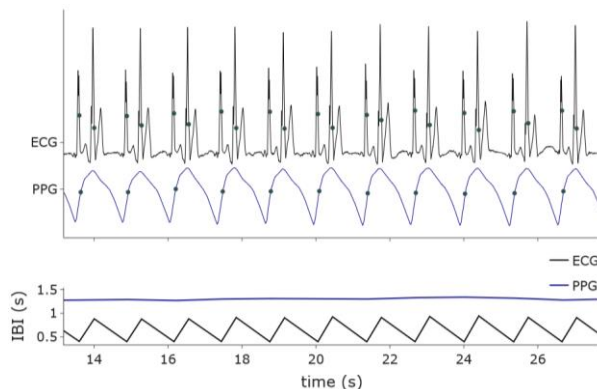


Figure 2. Example of bigeminy. Undetected PPG-beats result in a regular sequence of IBIs that is classified as normal.

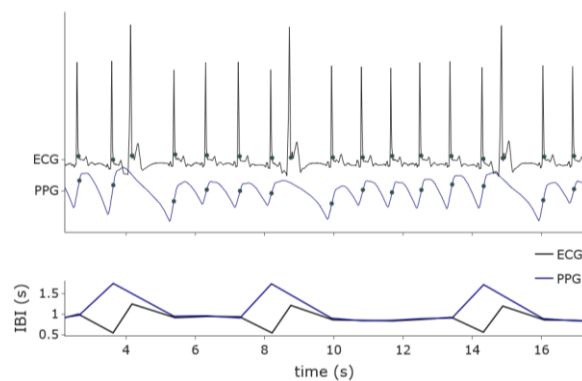


Figure 3. Example of extrasystoles. Extrasystoles have different patterns in IBIs extracted from ECG or PPG signals.

#### 5. Conclusion

This study shows the ability to detect not only AF but also other CAs, like atrial tachycardia, atrioventricular (nodal or not) re-entrant tachycardia and atrioventricular blocks, based on sequences of IBIs. However, some CAs, like atrial flutter and bigeminy can be difficult to detect based on IBIs alone. Considering PPG waveform

information in addition to IBIs appears to be a necessary step towards the continuous monitoring of CAs in everyday life.

## Acknowledgments

This research was funded by the Swiss National Science Foundation: ENHEART project (205321\_192020).

## References

- [1] C. W. Tsao *et al.*, “Heart Disease and Stroke Statistics—2023 Update: A Report From the American Heart Association,” *Circulation*, vol. 147, no. 8, pp. e93–e621, Feb. 2023, doi: 10.1161/CIR.0000000000001123.
- [2] S. Khurshid *et al.*, “Frequency of Cardiac Rhythm Abnormalities in a Half Million Adults,” *Circ Arrhythm Electrophysiol*, vol. 11, no. 7, Jul. 2018, doi: 10.1161/CIRCEP.118.006273.
- [3] R. W. Rho and R. L. Page, “Asymptomatic Atrial Fibrillation,” *Progress in Cardiovascular Diseases*, vol. 48, no. 2, pp. 79–87, Sep. 2005, doi: 10.1016/j.pcad.2005.06.005.
- [4] B. Gorenek (chair) *et al.*, “Device-detected subclinical atrial tachyarrhythmias: definition, implications and management—an European Heart Rhythm Association (EHRA) consensus document, endorsed by Heart Rhythm Society (HRS), Asia Pacific Heart Rhythm Society (APHRS) and Sociedad Latinoamericana de Estimulación Cardíaca y Electrofisiología (SOLEACE),” *EP Europace*, vol. 19, no. 9, pp. 1556–1578, Sep. 2017, doi: 10.1093/europace/eux163.
- [5] T. Pereira *et al.*, “Photoplethysmography based atrial fibrillation detection: a review,” *npj Digital Medicine*, vol. 3, no. 1, Art. no. 1, Jan. 2020, doi: 10.1038/s41746-019-0207-9.
- [6] L. M. Eerikäinen *et al.*, “Detecting Atrial Fibrillation and Atrial Flutter in Daily Life Using Photoplethysmography Data,” *IEEE Journal of Biomedical and Health Informatics*, vol. 24, no. 6, pp. 1610–1618, Jun. 2020, doi: 10.1109/JBHI.2019.2950574.
- [7] Neha, H. K. Sardana, N. Dogra, and R. Kanawade, “Dynamic time warping based arrhythmia detection using photoplethysmography signals,” *SIViP*, Feb. 2022, doi: 10.1007/s11760-022-02152-z.
- [8] S. Fallet, M. Lemay, P. Renevey, C. Leupi, E. Pruvot, and J.-M. Vesin, “Can one detect atrial fibrillation using a wrist-type photoplethysmographic device?,” *Med Biol Eng Comput*, vol. 57, no. 2, pp. 477–487, Feb. 2019, doi: 10.1007/s11517-018-1886-0.
- [9] Z. Liu *et al.*, “Multiclass Arrhythmia Detection and Classification From Photoplethysmography Signals Using a Deep Convolutional Neural Network,” *Journal of the American Heart Association*, vol. 11, no. 7, p. e023555, Apr. 2022, doi: 10.1161/JAHA.121.023555.
- [10] M.-Z. Poh *et al.*, “Diagnostic assessment of a deep learning system for detecting atrial fibrillation in pulse waveforms,” *Heart*, vol. 104, no. 23, pp. 1921–1928, Dec. 2018, doi: 10.1136/heartjnl-2018-313147.
- [11] B.-F. Wu, B.-J. Wu, S.-E. Cheng, Y. Sun, and M.-L. Chung, “Motion-Robust Atrial Fibrillation Detection Based on Remote-Photoplethysmography,” *IEEE Journal of Biomedical and Health Informatics*, vol. 27, no. 6, pp. 2705–2716, Jun. 2023, doi: 10.1109/JBHI.2022.3172705.
- [12] W. Zong, T. Heldt, G. B. Moody, and R. G. Mark, “An open-source algorithm to detect onset of arterial blood pressure pulses,” in *Computers in Cardiology, 2003*, Sep. 2003, pp. 259–262. doi: 10.1109/CIC.2003.1291140.
- [13] A. N. Vest *et al.*, “An Open Source Benchmarked Toolbox for Cardiovascular Waveform and Interval Analysis,” *Physiol Meas*, vol. 39, no. 10, p. 105004, Oct. 2018, doi: 10.1088/1361-6579/aae021.
- [14] L. Jeanningros *et al.*, “A Comparative Study on Detecting Heart Beats in Photoplethysmography Signals in Presence of Various Cardiac Arrhythmias,” in *CinC 2023*, Atlanta, USA, under review. [Online]. Available: <https://cinc2023.org/>
- [15] J. Van Zaen *et al.*, “Atrial Fibrillation Detection from PPG Interbeat Intervals via a Recurrent Neural Network,” in *2019 Computing in Cardiology (CinC)*, Sep. 2019, p. Page 1-Page 4. doi: 10.23919/CinC49843.2019.9005767.
- [16] Ary L. Goldberger *et al.*, “PhysioBank, PhysioToolkit, and PhysioNet | Circulation,” *Circulation*, vol. 101, no. 23, pp. 215–220, Jun. 2000, doi: <https://doi.org/10.1161/01.CIR.101.23.e215>.

Address for correspondence:

Fabian Braun.  
CSEM, Rue Jacquet-Droz 1, 2000 Neuchâtel, Switzerland.  
[fabian.braun@csem.ch](mailto:fabian.braun@csem.ch)